

Tracking Gene Expression after DNA Delivery Using Spatially Indexed Nanofiber Arrays

Timothy E. McKnight,^{*,†,‡,§} Anatoli V. Melechko,^{†,||} Dale K. Hensley,^{†,‡}
David G. J. Mann,[⊥] Guy D. Griffin,[#] and Michael L. Simpson^{†,‡,§,▼}

Molecular Scale Engineering and Nanoscale Technologies Research Group, Condensed Matter Sciences Division, Engineering Science and Technology Division, and Life Sciences Division, Oak Ridge National Laboratory, Oak Ridge, Tennessee 37831, and Department of Electrical and Computer Engineering, Center for Environmental Biotechnology, and Department of Materials Science and Engineering, University of Tennessee, Knoxville, Tennessee 37996

Received April 1, 2004

ABSTRACT

The penetration and residence of vertically aligned carbon nanofibers (VACNF) within live cell matrices is demonstrated upon substrates that incorporate spatially registered indices to facilitate temporal tracking of individual cells. Penetration of DNA-modified carbon nanofibers into live cells using this platform provides efficient delivery and expression of exogenous genes, similar to “microinjection”-styled methods, but on a massively parallel basis. Spatially registered indices on the substrate allow one to conveniently locate individual cells, facilitating temporal tracking of gene expression events. We describe fabrication and use of this gene delivery platform which consists of arrays of individual carbon nanofibers at 5- μm pitch within numerically indexed, 100- μm square grid patterns. Fabrication of these devices on silicon substrates enables mass production of 100 devices (5 mm²) per wafer, with each device providing over 800,000 nanofiber-based “needles” for cellular impalement and gene delivery applications.

Among the many methods that may be used to deliver DNA to a cell, perhaps the most straightforward is microinjection—the direct administration of naked DNA to the nuclear domain of a targeted cell.¹ Microinjection forcibly bypasses a cell’s *physical* barriers, the plasma and nuclear membranes, that limit successful gene delivery.² Microinjection can also circumvent many of the cell’s *chemical* barriers against DNA uptake, including extracellular, endosomal/lysosomal, and cytosolic degradation pathways that all limit the effectiveness of nonnuclear delivery techniques³ (i.e.; electroporation, sonoporation, lipofection, and precipitation methods). The physical nature of microinjection has promoted its use not only for mammalian studies, such as genetic manipulation of fertilized ova,⁴ but also for nonmammalian cell types that are recalcitrant to other transformation techniques, such as plant cells that present the additional barrier of a cell wall.⁵

Success with ultrafine micropipets (<100 nm tip diameters) has also been reported on prokaryotes and even targeted organelles.⁶ Microinjection is thus often considered a universal DNA delivery mechanism. The task of microinjection, however, is time-consuming and arduous as the precision of the method requires the targeting of an individual cell and typically its nuclear envelope using fragile micropipets, precise micromanipulators, and accurate dispensing of (typically) subpicoliter volumes of material.

Recently, carbon nanofibers have been demonstrated as a parallel DNA delivery platform, where arrays of vertically aligned carbon nanofibers (VACNFs) grown on a flat substrate provide for simultaneous microinjection-styled delivery of DNA to many cells.⁷ These nanofiber arrays are surface coated with DNA and are directly integrated with cells by simply pressing them into cellular matrices or by centrifuging suspensions of cells down onto the fiber array. The transfer mechanism is a direct penetration and introduction of DNA simultaneously into many cells. We have named this technique “impalefection” to denote transfection of cells by physical impalement with DNA-modified nanofibers. Since a nanofiber array is used for simultaneous gene delivery to many cells, this specific application is called

* Corresponding author. E-mail: mcknightte@ornl.gov; phone 1-865-574-5681; fax 1-865-576-2813.

† Molecular Scale Engineering and Nanoscale Technologies Research Group, ORNL.

‡ Condensed Matter Sciences Division, ORNL.

§ Engineering Science and Technology Division, ORNL.

|| Department of Electrical and Computer Engineering, UT.

⊥ Center for Environmental Biotechnology, UT.

Life Sciences Division, ORNL.

▼ Department of Materials Science and Engineering, UT.

“parallel impalefection”. Like microinjection, this approach has the potential of being very effective as nanofiber penetration/gene delivery can often extend beyond the degradative cytosolic regions of the cell and into the nuclear domain, where transcriptional activity occurs. However, conventional single element microinjection systems must be carefully inserted into a cell, dispensed, and then removed. In contrast, the substrate-based configuration of nanofiber arrays enables them to be integrated with cellular matrices and then *left in place* (i.e., retained and assimilated by the cells). This residence capability provides for many DNA delivery options that are not available using traditional microinjection approaches, including the ability to covalently tether DNA to the nanofiber scaffold and thus possibly provide higher levels of control over the fate of introduced genes.

The parallelism of impalefection facilitates the simultaneous genetic manipulation of many cells, and the residence mode of cells following the integration events enables the unprecedented potential to microscopically track these cells as individuals and cell groups. This tracking, however, must be conducted over multiple length scales, i.e., at cellular dimensions across the entire nanofiber array, which is typically a 5-mm square platform with a surface area over 1 million times larger than a single cell. This is further complicated by the need to physically remove the array from the microscope for incubation between imaging events. These requirements necessitate a platform that can provide an unambiguous scheme for physically locating a specific site (at cellular dimensions) upon the array. In this letter, we describe a complete platform that provides both the massive parallelism of arrays of individual nanofibers as well as a unique approach to spatially registered indices that facilitate temporal tracking of gene delivery events. In this implementation, dense regions of VACNFs are used to provide a near cellular-scale indexed grid pattern that not only provides unambiguous location of regions of the array but also assists in making the device more rugged during device handling and cell integration manipulations.

The gene delivery platforms discussed in this work consist of arrays of individual VACNFs. VACNFs are synthesized on silicon substrates in a dc-plasma enhanced chemical vapor deposition process from photolithographically defined patterns of nickel thin films.^{8–11} In this work, two subsequent catalyst patterning processes are used to define the fiber growth sites for both gene delivery elements and indexing grids. First, a silicon wafer is spin coated with SPR 955CM-0.7 resist (Shipley) at 6000 rpm for 60 s and subsequently baked at 90 °C for 90 s on a hotplate. A 5× reduction stepper is then used to expose a pattern across the wafer consisting of isolated 500 nm diameter circular regions (dots) at a 5 μm pitch. This pitch is comparable to the diameter of a typical unattached, mammalian cell. Following post-exposure baking at 120 °C for 90 s, development in CD-26 for 60 s, and a 30 s oxygen plasma etch to ash residual resist, the wafer is metallized with 50 Å of nickel using electron-gun physical vapor deposition at 10⁻⁶ Torr. Metal liftoff is performed by dissolving photoresist in acetone for 1 h, briefly ultrasonicating, and subsequently rinsing in acetone and

isopropyl alcohol, leaving 400-nm diameter nickel dots at a defined pitch across the wafer. The wafer is then spun with 1813 photoresist (Shipley) and contact photolithography is used to pattern the wafer with an indexing pattern, consisting mainly of 5-μm wide stripes at 100-μm intervals both horizontally and vertically across the wafer. These stripes define 100-μm square regions, inside of which are the individual nickel dots. In each 100-μm square, a unique *X* and *Y* numerical index is also lithographically defined to provide spatial registration marks in each square. Following development and a 30 s oxygen plasma etch, the wafer is again metallized with 100 Å of nickel, and liftoff is again performed. VACNFs are then synthesized in a dc-PECVD chamber using a mixture of acetylene and ammonia (3 Torr total pressure, 50 sccm of C₂H₂, 80 sccm of NH₃, 400 mA, and 520 V). During carbon nanofiber synthesis, each nickel dot catalyzes the formation of an individual VACNF. The horizontal and vertical stripes and numerical index patterns form more densely populated regions of nanofibers. The final product is a silicon wafer with a 10 × 10 array of 5-mm square gene delivery “chips”, where each chip consists of a 45 × 45 element array of uniquely indexed 100-μm squares. Each 100-μm square, in turn, contains an array of individual nanofiber elements (Figure 1). Thus, each 100-μm square contains approximately 400 individual nanofibers, and a single 5-mm chip provides ~800,000 parallel DNA delivering nanofibers. VACNFs are grown using parameters that provide sharp tips (<100-nm diameter) and lengths of several microns, both of which are important factors that facilitate penetration into a cell. Sharper tips induce less trauma to the cell during interfacing procedures and can penetrate cell walls and membranes if the length of the fibers is sufficient to overcome compliance of the cellular membrane. Typically, we grow nanofibers to approximately half the diameter of the cell being studied. Following synthesis, wafers are cleaved into individual chips using a diamond scribe.

Nanofiber array chips are surface treated with DNA prior to interfacing with cellular matrices. We have predominantly used two surface modification methods that we refer to as “spotting” and “covalent tethering”. Spotting refers to simply dispensing 1–3 μL volumes of DNA solution (100–1000 ng/μL in water) onto a 5-mm square chip and allowing the spot to dry. Covalent tethering is conducted using a carbodiimide-mediated condensation reaction (amidization) between DNA base amines and surface carboxylic acid groups on the fibers, as previously reported for both nanofibers and nanotubes.^{7,12} Spotting provides desorption of DNA from the fibers within the intracellular domain. Tethering immobilizes DNA to the nanofibers and appears to retain the DNA on the nanofiber while still allowing some transcription of the tethered genes.

Sterilization of nanofiber array chips is required to avoid infection of cell cultures. Following VACNF surface treatment with DNA, chips are typically sterilized by soaking in both acetone and ethanol. Both of these reagents will dehydrate DNA onto the nanofiber surface but do not appear to significantly impact subsequent expression of the delivered

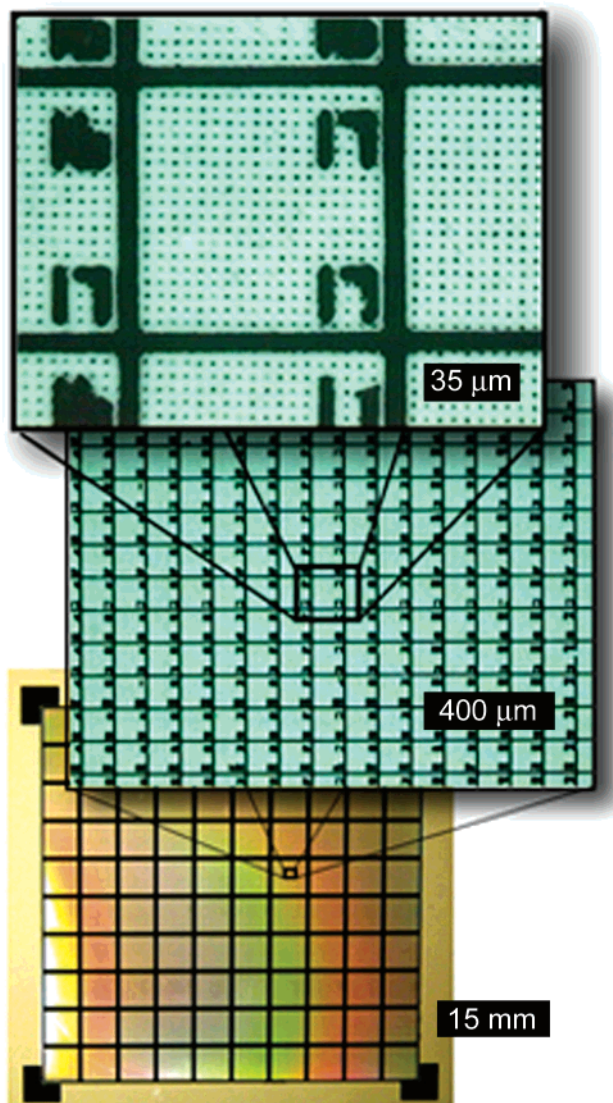


Figure 1. Three optical micrographs of spatially indexed nanofiber gene delivery arrays. (Bottom) Cutout view of a 4-in. diameter silicon wafer upon which has been fabricated a 10×10 array of 5-mm square DNA delivery chips. (Middle) Each chip contains a 45×45 array of numerically indexed $100\text{-}\mu\text{m}$ square grids. These in turn contain individual nanofibers at a pitch optimized for the type of cell line being evaluated. Here the pitch between nanofibers is set at $5\text{-}\mu\text{m}$ (top).

genes (data not shown). Autoclaving of chips may also be performed prior to DNA modification if the subsequent modification is performed using sterile reagents. Antibiotic supplement of cultures is an option but should only be used as necessary in order to avoid the development of antibiotic resistance of infectious contaminants. Acetone/ethanol sterilized chips have been used successfully with mammalian cell culture for extended periods (at least 4 weeks) without the use of antibiotics.

Cells are interfaced to DNA modified nanofiber arrays using several methods. To date, the most effective method is to centrifuge suspensions of cells onto nanofiber arrays and to subsequently sandwich the pelleted cells between the array chip and a sterilized, flat, compliant surface, such as a flat expanse of sterile poly(dimethylsiloxane) (PDMS, Syl-

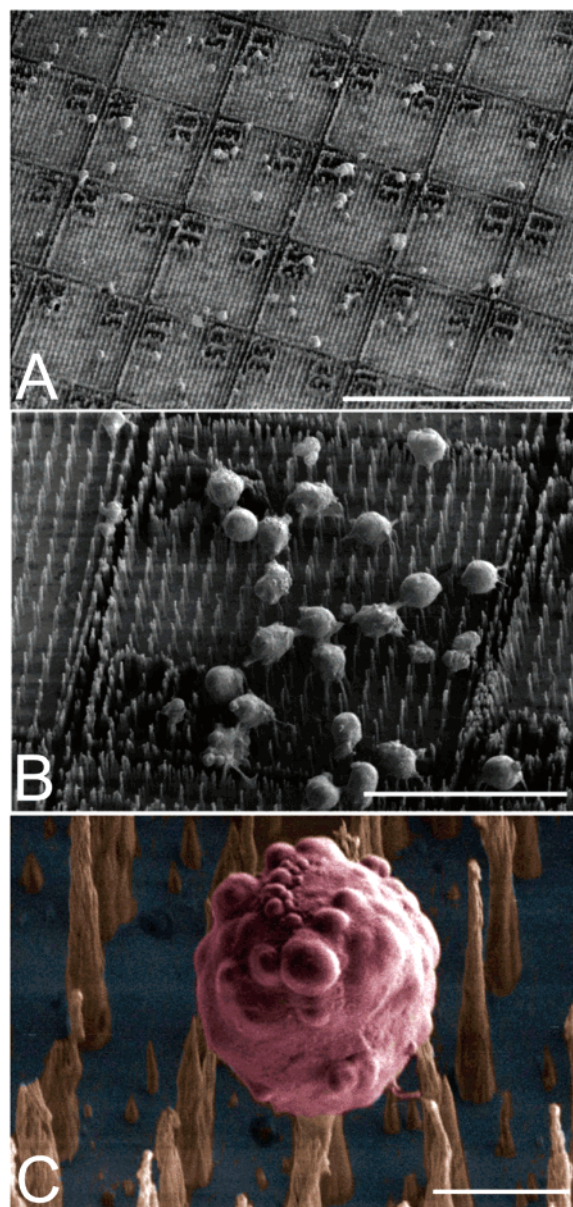


Figure 2. Electron micrographs of mammalian cells (SP2/0-AG14; mouse myeloma¹³) following centrifugation at 600G onto an indexed nanofiber gene delivery chip and culture for 3 days (viewing angle is 30 degrees). Scale bars: A = $200\ \mu\text{m}$, B = $50\ \mu\text{m}$, C = $5\ \mu\text{m}$. Cells were fixed with 2% glutaraldehyde in PBS and dehydrated with methanol prior to electron microscopy. SP2 cells were used for this image as they are a suspension cell line and therefore do not attach and spread on the nanofiber platform, thus facilitating clearer images. Nonetheless, some material has clearly agglomerated onto the fiber surfaces, as seen in panel C (false color added).

gard 184, Dow Corning). For mammalian cells, 0.5 mL of cells are suspended in isotonic phosphate buffered saline (PBS) at variable density and are centrifuged onto the fibers at 600G for 1 min (Figure 2). The cell-covered chip is then placed face down on a PDMS film and the backside of the chip is gently pressed with sterile forceps. The chip is then placed face up in growth media to allow cell recovery and proliferation on the nanofiber array platform. Alternatively, the centrifugation step may be bypassed by simply dispensing cell suspensions onto nanofiber chips and allowing cells to

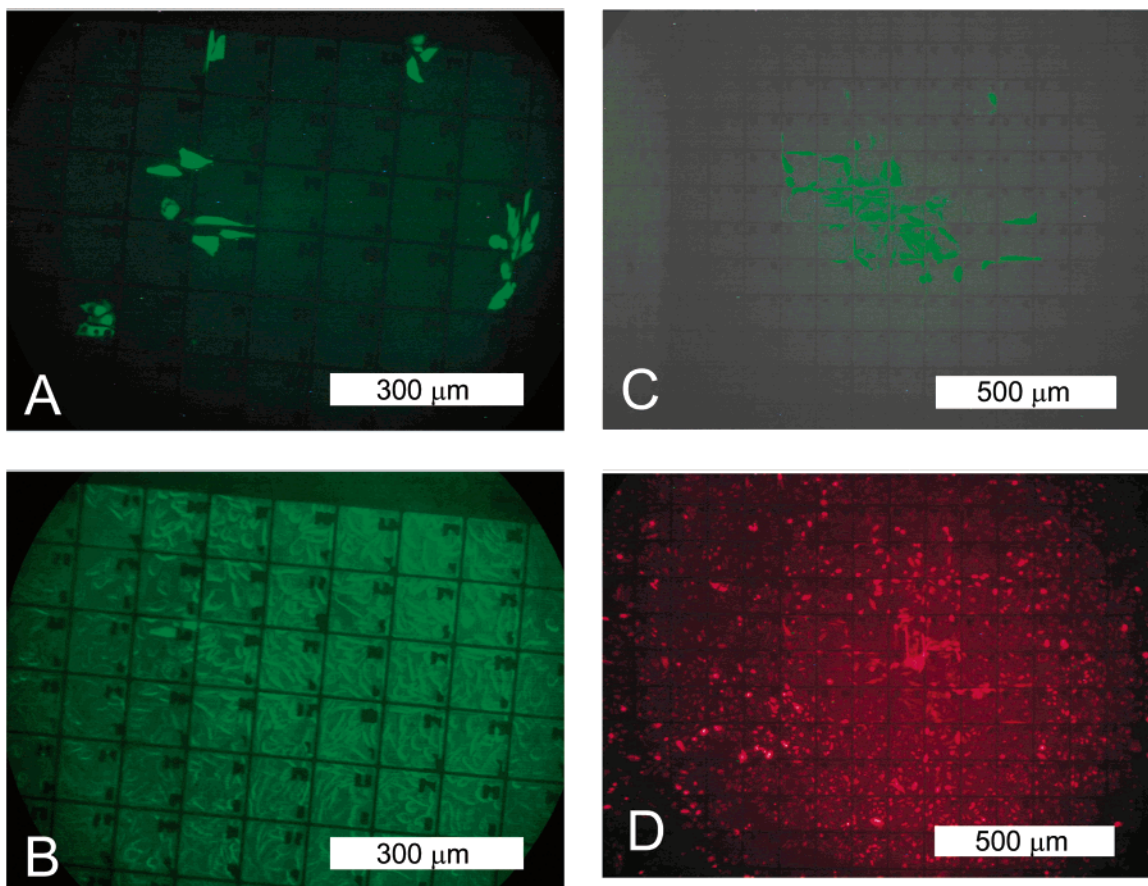


Figure 3. 488 nm (A) and white light excited (B) images of YFP expression in CHO cells 36 h following impalefection. YFP expression can clearly be distinguished from any native fluorescence (autofluorescence) of the CHO cells. (C) YFP expression from a colony or colonies of YFP-expressing cells 10 days following impalefection and 7 days into selection using the antibiotic G418. (D) Uptake of propidium iodide by neighboring nontransformed cells provides evidence that antibiotic selection is killing nontransformed cells. The YFP-expressing colony, however, has maintained normal spindle shaped morphologies and continues to proliferate through the antibiotic selection.

settle out of suspension prior to sandwiching them against the chip on a flat surface.

The results of a DNA delivery experiment conducted using spatially indexed nanofiber arrays are presented in Figure 3. A constitutively expressed yellow fluorescent protein (YFP) under the human cytomegalovirus immediate early promoter-(CMV_{IE}) reporter plasmid (pd2EYFP-N1, Clontech) was covalently tethered to indexed nanofiber array chips using 500 μ L of 100 mM MES buffer at pH 4.8 with 5 mg 1-(3-dimethylaminopropyl)-3-ethylcarbodiimide (EDC) and 400 ng of plasmid DNA for each chip. In parallel, control chips were prepared by excluding the YFP plasmid DNA from the reaction mix. The reactions were incubated overnight on a rocker at 25 °C, followed by quick rinsing with PBS and deionized water prior to acetone/ethanol sterilization. Chinese hamster ovary cells (CHO K₁BH₄^{14,15}) were interfaced to nanofiber chips by dispensing 50 μ L of a \sim 200,000 cell/mL cell suspension in PBS, waiting 5 min, and sandwiching the cells on the chip against a flat surface of PDMS. This achieved seeding of a few cells per 100- μ m square grid upon the nanofiber chips. Following a recovery period of 36 h, epifluorescent images using a GFP filter (488ex:510em) were captured using an eyepiece mounted, true color, digital camera to record YFP expression in interfaced cells and their

progeny. Figure 3 presents a 488 nm (A) and a white light (B) excitation image that provides for comparison of YFP-expressing cells against other nonexpressing cells on the chip at 36 h post-impalefection. YFP expression in cells can clearly be distinguished from autofluorescence of cells, as the enhanced GFP variants now available have very high extinction coefficients and are therefore very bright with respect to the autofluorescence of most cultured cells. Control samples, where the YFP plasmid was not added to the EDC reaction mixture, resulted in no such fluorescence. In Figure 3A, six local regions of cells are observed to be expressing YFP, and these groups are surrounded by nonexpressing cells upon the nanofibered substrate. Impalefection efficiencies (# of expressing cells/# of total cells on the chip) are variable, perhaps largely due to the variability that the press step imparts. In addition to dependence on the press step, efficiency of gene delivery appears to be dependent on factors such as fiber tip diameter and morphology, although further tests are necessary to verify. In this test, fiber diameters were approximately 200 nm and efficiency was less than 5% based on the total number of cells on the chip.

Figure 3C presents a colony or colonies of pd2EYFP-N1 expressing CHO cells on another chip of this experimental set at day 10 post-impalefection. In addition to encoding

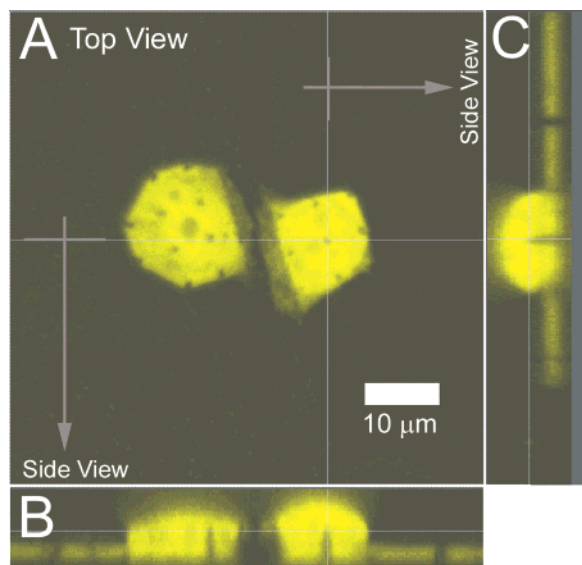


Figure 4. Laser scanning confocal image of two YFP-expressing impalefected CHO cells. The images at bottom (B) and on the right (C) are derived from a stack of images acquired from scans parallel to the substrate. In the top-view image (A), nanofibers are seen as distinct dark circles within the cells. In the images at the bottom (B) and right (C), the penetrant nanofibers within the cells can clearly be distinguished as elongated, dark regions. The dark area between the two cells is a fiber wall that defines one of the 100 μm square indexing grids.

YFP, the pd2EYFP-N1 plasmid hosts a neomycin/kanamycin resistance gene of Tn5 under the SV40 early promoter, thus enabling for selection of stably transfected eukaryotic cells using the antibiotic, G418. At day 3+, G418 was applied and maintained on this sample at a concentration of 300 $\mu\text{g}/\text{mL}$. Over the next week, non-YFP-expressing (wild type) cells on this chip lost their nominal spindle-shaped morphology and rounded upon the fibered substrate, but did not become unattached even with forced rinsing, perhaps due to fiber impalement. At day 10, propidium iodide was added to the sample at a final concentration of 1 μM . This dye can be used as a cell viability stain, where healthy cells can exclude this dye but compromised or dead cells will uptake the dye resulting in intense fluorescence due to dye intercalation into nucleic acids. Figure 3D presents the same region of the chip as shown in Figure 3C following incubation in propidium iodide (PI) for 10 min (TRITC filter set). Here, the surrounding non-YFP-expressing cells show clear uptake of PI, indicating that their membranes are compromised and cell death has occurred or is eminent. In contrast, the YFP-expressing cells have withstood the G418 selection as evidenced by their normal spindle shaped morphology, continued proliferation, and their ability to exclude PI. The slight red fluorescence observed from these YFP-expressing cells is due to strong expression of YFP, which has emission spectra that extend into the wavelengths observed with the TRITC filter set. This emission was observed in these cells prior to PI application and did not appear to significantly change upon addition of the dye.

Figure 4 presents a laser scanning confocal image of two YFP-expressing, impalefected CHO cells on another chip

from the same experiment. At the bottom and at right, profile images of the cells are shown, derived from cross sections of a stack of 35 scans over a region from $\sim 8 \mu\text{m}$ above the nanofiber substrate to the substrate surface. In these side view images, the nanofibers can clearly be discriminated as extending deeply into the impaled cells. The dark, linear region between the two cells is a wall of fibers that defines the nanofiber-based indexing pattern.

Figure 5 presents a time lapse series of GFP expression in CHO cells over a period of 170 h following impalefection. For this experiment, chips were covalently modified with the pGreenLantern-1 plasmid (formerly available from Gibco BRL), a reporter plasmid with green fluorescent protein expression (GFP) under the CMV_{IE} promoter. The covalent modification was performed as above, but the chips were extensively washed in water and PBS following amidization, prior to sterilization. Cells were interfaced to chips by using a centrifugation and press protocol, where a very dilute solution of cells was used such that the seeding density would be light enough to allow extensive cell proliferation on the chip (approximately hundreds of cells per 25 mm^2 chip). Imaging began at 48 h, and chips were maintained in growth media in an incubator between each imaging event. The grid pattern and numerical indices evident in these images allowed unambiguous identification and tracking of cells on the 5-mm square chip for each imaging event, as well as tracking of other cell groups on the same chip. On the chip presented in Figure 5, two of 14 isolated groups of cells tracked over the 7 day period are shown.

In the top sequence, where a cell group in region [15,25] of the array is tracked, gene delivery to one or possibly a few recipient cells resulted in the formation of a large colony of cells, all of which express the exogenous gene, producing GFP. There are several possible explanations for formation of such a GFP expressing colony. If enough copies of the plasmid were delivered, transient expression may occur both within recipient impaled cells as well as within those progeny that receive segregated plasmid during division. However, segregation can occur only if the plasmid DNA is free to disassociate from the fibers. The DNA on this sample was covalently tethered and therefore should not be free to disassociate. Nonetheless, it is possible that some residual nontethered DNA remained on the fibers throughout the rinsing and sterilization procedure. More often, however, extensive rinsing successfully removes unbound DNA from our nanofiber samples. Alternatively, and perhaps more likely, the GFP-expressing cluster may actually be a demonstration of stable genomic insertion of the plasmid gene. Here, bound or unbound plasmid may have interacted with the host cell's chromosomal DNA, resulting in a recombination event where the plasmid gene became stably inserted into the host genome. Progeny cells of this cell would thus inherit the GFP gene, forming a GFP-expressing clonal colony. Studies with conventional nuclear microinjection into CHO have demonstrated that the frequency of stable genomic insertion of plasmid DNA via nonhomologous recombination can be as high as 10% for cells that receive multiple copies of plasmid to their nuclear domain.¹⁶ Verification that this

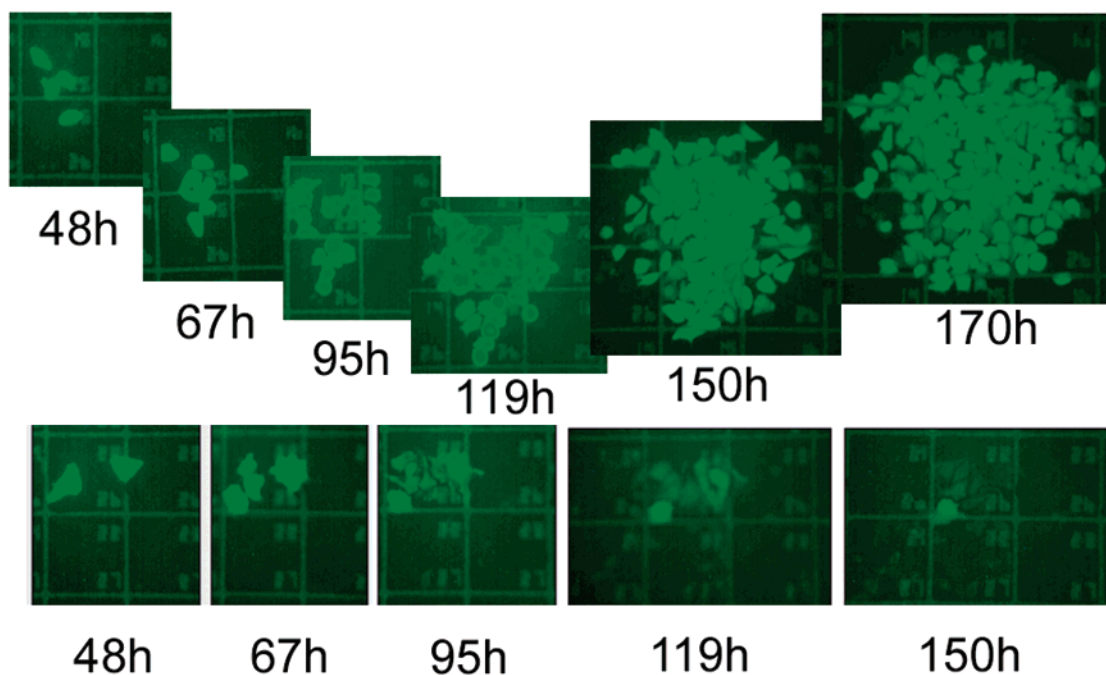


Figure 5. Two examples of nanofiber-mediated gene delivery and expression in cells proliferating on a spatially indexed nanofiber array. The spatial indexing pattern seen in each image allows one to locate the same region of the chip for fluorescent imaging. Numbers in each image refer to the elapsed time (in hours) since impalefection.

is indeed occurring within impalefected cells, however, requires further analysis.

In the bottom sequence of Figure 5, where cells within the [22,26] region of the array are tracked, GFP is expressed by one or two cells during a 6 day period, but the progeny of these cells do not appear to express GFP. Rather, it appears that progeny cells receive a portion of their progenitor cell's GFP, and this aliquot of protein decays over time. This scenario occurred in 5 of the 14 groups tracked on this sample, with the remaining groups ceasing GFP expression entirely within the first few days of the experiment. A possible explanation is that transient expression of tethered plasmid is limited to only those cells that remain impaled on nanofibers and which putatively maintain nuclear presence of the nanofiber and therefore transcriptional access to the nanofiber-bound plasmid. Progeny cells grow on and around nanofibers, including over the nanofibered grid patterns, but progeny cells are typically *not* impaled (data not shown). Therefore, these nonimpaled progeny cells receive a dose of the GFP *protein* during cell division of their impaled progenitor cell, but are unable to produce more as they have no access to the tethered *plasmid*. With time, GFP content in progeny decays due to protein degradation within the cell, as seen by reduction of green fluorescence in these cells at 95, 119, and 150 h. Cells that remain impaled, however, can continue to produce GFP. In other experiments, GFP production from tethered plasmids has continued for as long as four weeks in some cells, at which time, expression was still maintained but the experiments were terminated.

The temporal tracking provided by these indexed gene delivery platforms has revealed differences in cell division rates of impaled vs nonimpaled cells. For example, by observing the proliferation of GFP-expressing cells in the top sequence of Figure 5, it can be observed that nonimpaled

progeny cells have a clonal growth rate of approximately 20–24 h per division. While this is longer than the 14 h clonal growth rate of wild-type CHO, decreased cell proliferation can occur due to a number of factors, including differences in adherence to the growth substrate, the high metabolic load imposed upon the cell by overexpression of any gene from a strong viral promoter (such as CMV_{IE}), and the high levels of GFP that are expressed. More marked, however, is that the GFP-expressing and putatively *impaled* cell in the bottom sequence appears to have experienced only one or two divisions during the 6-day experiment. It is established that conventional protonuclear microinjection can detrimentally impact cell development immediately following the microinjection event.⁴ However, subsequent development following removal of the microinjection capillary appears to continue normally after a period of cell recovery. We are currently investigating if *continued* nanofiber residence within a cell may be impacting division mechanisms using these indexed array platforms. Also, it is of interest that following division of an impaled cell, putative nuclear presence of a nanofiber is often maintained, as evidenced by continued expression of the tethered plasmid in some cells following mitosis. If so, it is critical to understand what mechanisms are involved in preserving fiber residence within the nuclear domain, even apparently following mitotic events such as prometaphase nuclear membrane breakdown and telophase nuclear membrane reformation. Spatially indexed nanofiber array platforms provide a unique opportunity to continue to study these phenomena.

We have demonstrated that arrays of vertically aligned carbon nanofibers can be used effectively to deliver genes to cellular matrices and that this system can be configured with spatially indexed registration marks that facilitate the tracking of gene delivery events and cell proliferation on

the nanofiber platform. We anticipate that use of these platforms for *impalefection*, a mechanically based, micro-injection-styled approach, will enable observation of gene expression phenomena across a broad range of cell types. Ultimately, the simplicity of using this platform and the ability to tether genes to the carbon nanofiber scaffolding may open new possibilities for studying and manipulating gene expression events and for developing genetically manipulated whole cell biosensing and actuating systems.

Acknowledgment. The authors thank J. Morrell for assistance with plasmid isolation and confocal microscopy, P. H. Fleming for assistance with metal depositions, and D. Austin and T. Subich for layout of the indexing mask. This work was supported in part by the National Institute for Biomedical Imaging and Bioengineering under assignment 1-R01EB000433-01, by the Material Sciences and Engineering Division Program of the DOE Office of Science under contract DE-AC05-00OR22725 with UT-Battelle, LLC and through the Laboratory Directed Research and Development funding program of the Oak Ridge National Laboratory, which is managed for the U.S. Department of Energy by UT-Battelle, LLC.

References

- (1) Luo, D.; Saltzman, W. M. *Nature Biotechnology* **2000**, *18*, 33.
- (2) Segura, T.; Shea, L. D. *Annu. Rev. Mater. Res.* **2001**, *31*, 25.

- (3) James, M. B.; Giorgio, T. D. Nuclear associated plasmid, but not cell associated plasmid, is correlated with transgene expression in cultured mammalian cells. *Molecular Therapy* **2000**, *1*, 339.
- (4) Perua, T. T.; Tolvanen, M.; Hyttiren, J. M.; Jaenne, J. *Theriogenology* **1995**, *43*, 1087.
- (5) Neuhaus, G.; Spangenberg, G. *Physiol Plant* **1990**, *79*, 213.
- (6) Knoblauch, M.; Hibberd, J. M.; Gray, J. C.; van Bel, A. J. E. *Nature Biotechnol.* **1999**, *17*, 906.
- (7) McKnight, T. E.; Melechko, A. V.; Griffin, G. D.; Guillorn, M. A.; Merkulov, V. I.; Serna, F.; Hensley, D. K.; Doktycz, M. J.; Lowndes, D. H.; Simpson, M. L. *Nanotechnology* **2003**, *14*, 551.
- (8) Merkulov, V. I.; Melechko, A. V.; Guillorn, M. A.; Simpson, M. L.; Lowndes, D. H. *Appl. Phys. Lett.* **2001**, *79*, 2970.
- (9) Merkulov, V. I.; Guillorn, M. A.; Simpson, M. L.; Lowndes, D. H.; Voekl, E. *Appl. Phys. Lett.* **2001**, *29*, 1178.
- (10) Merkulov, V. I.; Hensley, D. K.; Melechko, A. V.; Guillorn, M. A.; Lowndes, D. H.; Simpson, M. L. *J. Phys. Chem. B* **2002**, *106*, 10570.
- (11) Melechko, A. V.; McKnight, T. E.; Hensley, D. K.; Guillorn, M. A.; Merkulov, V. I.; Lowndes, D. H.; Simpson, M. L. *Nanotechnology* **2003**, *14*, 1029.
- (12) Dwyer, C.; Guthold, M.; Falvo, M.; Washburn, S.; Superfine, R.; Erie, D. *Nanotechnology* **2002**, *13*, 601.
- (13) For further cell description and culture information, please see the DSMZ-Deutsche Sammlung von Mikroorganismen und Zellkulturen at <http://www.dsmz.de/mutz/mutz146.htm>.
- (14) For culture information, compare to American Type Cell Culture Strain CCL-61 at <http://www.atcc.org/SearchCatalogs/longview.cfm?view=ce,401086,CCL-61&text=CHO&max=20>.
- (15) Hsie, A. W.; Casciano, D. A.; Couch, D. B.; Krahn, D. F.; Oneill, J. P.; Whitfield, B. L. *Mutation Res.* **1981**, *86*, 193.
- (16) Proctor, G. N. *Methods Mol. Cell Biol.* **1992**, *3*, 209.

NL049504B